A Numerical Investigation of TBA.....!!!1

By H.G.K.G Jayatunga

A thesis submitted to Monash University in fulfilment of the requirements for the Degree of

Doctor of Philosophy

Department of Mechanical Engineering
Monash University
Date ...!!!!!!

Contents

Chapter 1

A review of the literature

1.1 Flow induced vibrations

1.2 Fluid-elastic galloping

Fluid-elastic galloping is one of the most commonly observable flow-induced vibration on a slender body. Since this phenomenon is most common in civil structure, such as buildings and iced-transmission lines, the term "aeroelastic galloping" is commonly used as the body is immersed in air. However, this mechanism can occur on a slender body immersed in any Newtonian fluid, provided that the conditions to sustain the galloping mechanism are satisfied. This work is based on a general Newtonian flow,thus the term " fluid-elastic galloping" is used throughout this thesis.

1.2.1 Excitation of galloping

Païdoussis et al. (2010) describes galloping as a "velocity dependent and damping controlled" phenomenon. Therefore, in order for a body to gallop, an initial excitation has to be given to that body. While this excitation is mainly caused by the force crated from vortex shedding, other fluid instabilities may contribute to this initial excitation. When a bluff body moves along the transverse direction of the fluid flow, it generates a force along the transverse direction. This force, also known as the induced lift is a resultant of the velocity of the fluid and the motion of the body. When this body is attached to an

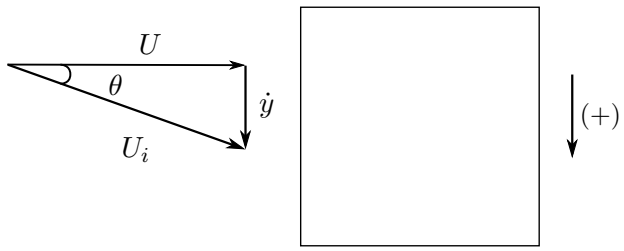

Figure 1.1: Induced angle of attack on the square prism due to the resultant of free-stream velocity of the fluid and transverse velocity of the body.

oscillating system (i.e. a simple spring, mass and damper system), the induced lift becomes the periodic forcing of the system. Galloping is sustained if the induced lift is in phase with the motion of the body. This could be explained further by using a square cross section as an example.

Figure 1.1 illustrates the motion of the body at a given instantaneous time.The induced angle of attack is formed on the square cross section as a result of the fressrteam velocity vector U and the transverse velocity vector of the body $\dot{y}$. Thus, a force is formed in phase with the motion of the body (square cross section). This mechanism could also be observed on other bodies which are prone to galloping. The sign convention in this figure (and generally used in this scope of research) states that downward direction is positive. Hence, the force generated on a body under the influence of galloping, could be also identified as a "negative lift".

1.2.2 Quasi-steady state theory

According Païdoussis et al. (2010),the initial studies by Glauert (1919) provided a criterion for galloping by considering the auto-rotation of a stalled aerofoil. As this phenomenon commonly occur in iced transmission lines, Den Hartog (1956) has provided a theoretical explanation for iced electric transmission lines.

The pioneering study in order to mathematically model galloping was conducted by Parkinson and Smith (1964). This model has been widely used in almost all subsequent studies regarding galloping. A weakly non-linear oscillator model was developed by them to predict the response of the system. Essentially the quasi-steady assumption was made to develop this theory assuming that the instantaneous induced lift force of the oscillating

body is equal to that of the lift force generated by the same body at the same induced angle of attack. In order to satisfy the quasi-steady assumption few conditions had to be satisfied.

- The velocity of the body does not change rapidly
- There is no interaction between vortex shedding and galloping

The second condition is satisfied by ensuring the vortex shedding frequency is much higher than the galloping frequency. The oscillator equation was solved using the Krylov and Bogoliubov method. Details of this method would not be mentioned as it is not used in the present study to solve the oscillator equation. The results obtained form experiments, carried out at $Re = 2200$ and a mass ratio (m^*) around 1164 had a good agreement with the theoretical data which is shown in figure 1.2.

Quasi-steady state oscillator model

The equation of motion of transversely oscillating body is given by

$$m\ddot{y} + c\dot{y} + ky = F_y, \tag{1.1}$$

where the forcing term F_y is given by

$$F_y = \frac{1}{2}\rho U^2 \mathcal{A} C_y. \tag{1.2}$$

As explained previously, when quasi-steady assumption is used the stationary C_y data (which consists of both lift and drag data) of the body could be could be used as inputs to the oscillator equation.Parkinson and Smith (1964) used a 7^th order odd interpolating polynomial to determine C_y. The order of the polynomial can be chosen arbitrarily depending on the study. For example Barrero-Gil et al. (2009, 2010) have used a 3_{rd} order polynomial in order to simplify the analytical model. However, Ng et al. (2005) pointed out that a 7_{th} order polynomial is sufficient as it does not provide a significantly better result.

$$C_y(\theta) = a_1\left(\frac{\dot{y}}{U}\right) - a_3\left(\frac{\dot{y}}{U}\right)^3 + a_5\left(\frac{\dot{y}}{U}\right)^5 - a_7\left(\frac{\dot{y}}{U}\right)^7. \tag{1.3}$$

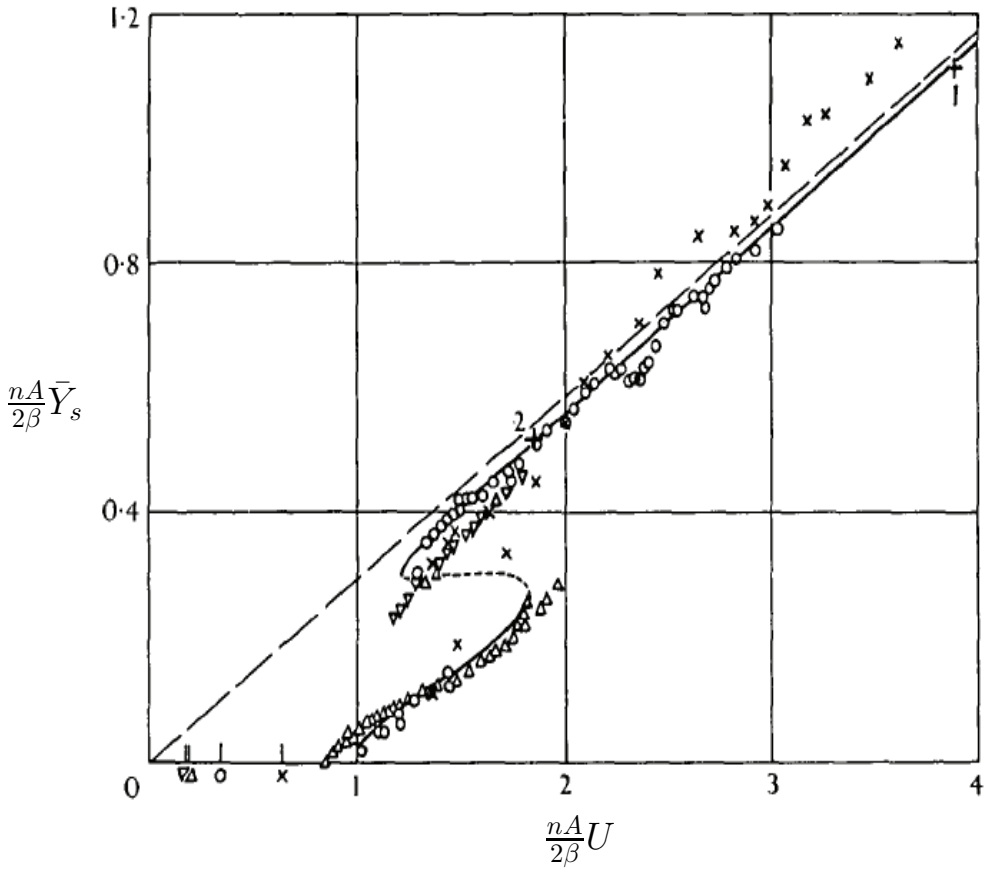

Figure 1.2: "Collapsed amplitude-velocity characteristic. Theory: ——— stable limit cycle, - - - unstable limit cycle. Experiment $\times$ $\beta = .00107$, $\circ$ $\beta = .00196$, $\triangle$ $\beta = .00364$,$\triangledown$ $\beta = .00372$, $+1$ $\beta = .0012$, $+2$ $\beta = .0032$ Reynolds numbers $4,000 - 20,000$ ". Figure extracted from Parkinson and Smith (1964). $\frac{nA}{2\beta}\bar{Y}_s$ is the dimensionless displacement amplitude parameter and $\frac{nA}{2\beta}U$ is the reduced velocity.

Therefore by substituting the forcing function to the oscillator equation (Eq:1.1) the Quasi-steady state (QSS) model could be obtained (Eq:1.4).

$$m\ddot{y}+c\dot{y}+ky=\frac{1}{2}\rho U^2\mathcal{A}\left(a_1\left(\frac{\dot{y}}{U}\right)-a_3\left(\frac{\dot{y}}{U}\right)^3+a_5\left(\frac{\dot{y}}{U}\right)^5-a_7\left(\frac{\dot{y}}{U}\right)^7\right). \tag{1.4}$$

As the current study is focused on the low Reregion, it is a known fact that the vortex shedding will be correlated well and therefore provide a significant forcing in the low Reynolds number region. Joly et al. (2012) introduced and additional sinusoidal forcing function to the model in order to integrate the forcing by vortex shedding. By the addition of this forcing Joly et al. (2012) managed to obtain accurate predictions of the displacement amplitude even at low mass ratios, where the galloping is suppressed or not present. Yet, the strength or the amplitude of this sinusoidal forcing has to be tuned in an *ad hoc* manner, and it was not clear the relationship between this forcing with the other system parameters. Thus in the current study this forcing was not used.

Presence of hysteresis

Hysteresis could be observed in the in the amplitude data of Parkinson and Smith (1964). In contrast, the studies carried out by Barrero-Gil et al. (2009) and Joly et al. (2012) at much lower Reynolds numbers ($159 \geq Re \leq 200$), did not show any hysteresis. Luo et al. (2003) concluded that the hysteresis was present due to the presence of an inflection point in the C_y curve at high Reynolds numbers (Parkinson and Smith (1964) data) which was not present at lower Reynolds numbers. It was further explained and demonstrated by Luo that the inflection point occurs due to the intermittent re attachment of the shear layer in certain angles at high Reynolds numbers.

1.2.3 Induced force and the shear layers

It is important to have an understanding on how the induced lift is generated in a fluid dynamics point of view. Since the quasi-steady model has already been validated and revalidated by many studies, the flow-field data of static body simulations could be used to analyse the underpinning fluid dynamic mechanisms governing galloping.

The governing mechanism of galloping is the behaviour of the shear layers on the top and bottom of the body. A common example is a square cross section which has been used

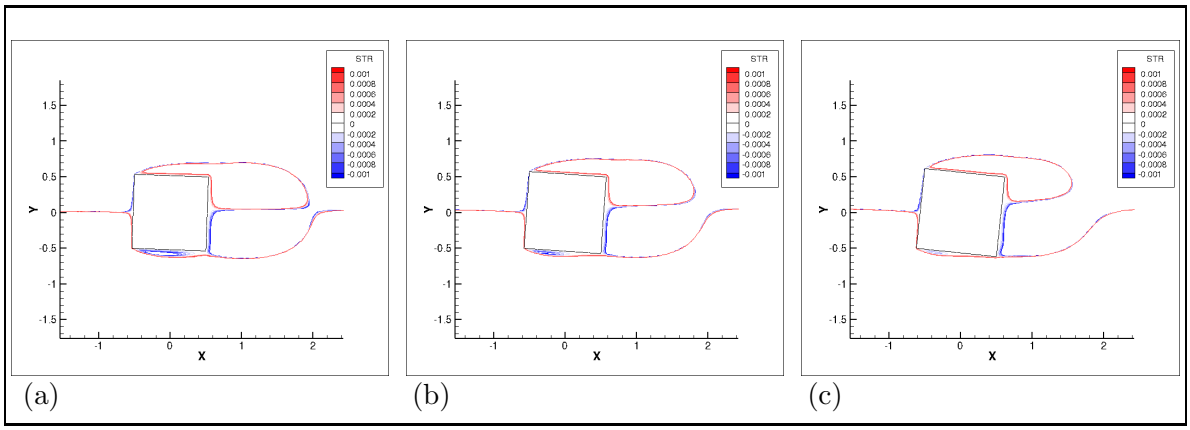

Figure 1.3: Stream functions of time averaged flow field on a stationary square section at $Re = 200$ at different incidence angles. (a) 2° (C_y increases),(b) 4° (C_y peaks) and (c) 2° (C_y decreases). The bottom shear layer comes closer to the bottom wall and reattaches as the angle of incidence increase.

widely in studies on galloping. In this square cross section (figure 1.3) the flow separate from the leading edges of the body and create two shear layers on the top and bottom sides of the the body. Figure 1.3 shows the stream functions of time averaged (over a vortex shedding cycle) flow fields of a stationary cross sections. The angle of incidence increases clockwise from $2^\circ - 6^\circ$. As θ is increased, the bottom shear comes closer to the wall of the body compared to the top shear layer (Figure 1.3 (a)). The shear layer nearer to the body crates higher suction compared to the shear layer at the opposite side. This pressure imbalance between the top and bottom sides of the body creates a downward force (i.e. the negative lift). As the angle is increased, the bottom shear layer becomes more closer and therefore the pressure difference becomes grater leading to a higher C_y. The negative lift force becomes maximum when the shear layer near to the wall reattaches at the trailing edge (figure 1.3 (b)). As θ is further increased, the bubble in the bottom shear layer shrinks in size resulting the reduction of the pressure imbalance of the top and bottom surface leading to the reduction in C_y. put the cY curve as crodd reference

1.2.4 Frequency response

Bibliography

Barrero-Gil, A., Alonso, G., Sanz-Andres, A., Jul. 2010. Energy harvesting from transverse galloping. Journal of Sound and Vibration 329 (14), 2873–2883.

Barrero-Gil, A., Sanz-Andrés, A., Roura, M., Oct. 2009. Transverse galloping at low Reynolds numbers. Journal of Fluids and Structures 25 (7), 1236–1242.

Bernitsas, M. M., Ben-Simon, Y., Raghavan, K., Garcia, E. M. H., 2009. The VIVACE Converter: Model Tests at High Damping and Reynolds Number Around 10[sup 5]. Journal of Offshore Mechanics and Arctic Engineering 131 (1), 011102.

Bernitsas, M. M., Raghavan, K., Ben-Simon, Y., Garcia, E. M. H., 2008. VIVACE (Vortex Induced Vibration Aquatic Clean Energy): A new concept in generation of clean and renewable energy from fluid flow. Journal of Offshore Mechanics and Arctic Engineering 130 (4), 041101–15.

Bouclin, D. N., 1977. Hydroelastic oscillations of square cylinders. Master's thesis, University of British Columbia.

Den Hartog, J. P., 1956. Mechanical Vibrations. Dover Books on Engineering. Dover Publications.

Glauert, H., 1919. The rotation of an aerofoil about a fixed axis. Tech. rep., Advisory Committee on Aeronautics R and M 595. HMSO, London.

Joly, A., Etienne, S., Pelletier, D., Jan. 2012. Galloping of square cylinders in cross-flow at low Reynolds numbers. Journal of Fluids and Structures 28, 232–243.

Lee, J., Bernitsas, M., Nov. 2011. High-damping, high-Reynolds VIV tests for energy harnessing using the VIVACE converter. Ocean Engineering 38 (16), 1697–1712.

Luo, S., Chew, Y., Ng, Y., Aug. 2003. Hysteresis phenomenon in the galloping oscillation of a square cylinder. Journal of Fluids and Structures 18 (1), 103–118.

Ng, Y., Luo, S., Chew, Y., Jan. 2005. On using high-order polynomial curve fits in the quasi-steady theory for square-cylinder galloping. Journal of Fluids and Structures 20 (1), 141–146.

Païdoussis, M., Price, S., de Langre, E., 2010. Fluid-Structure Interactions : Cross-Flow-Induced Instabilities. Cambridge University Press.

Parkinson, G. V., Smith, J. D., 1964. The square prism as an aeroelastic non-linear oscillator. The Quarterly Journal of Mechanics and Applied Mathematics 17 (2), 225–239.

Raghavan, K., Bernitsas, M., Apr. 2011. Experimental investigation of Reynolds number effect on vortex induced vibration of rigid circular cylinder on elastic supports. Ocean Engineering 38 (5-6), 719–731.

Vicente-Ludlam, D., Barrero-Gil, A., Velazquez, A., 2014. Optimal electromagnetic energy extraction from transverse galloping. Journal of Fluids and Structures 51, 281–291.

Vio, G., Dimitriadis, G., Cooper, J., Oct. 2007. Bifurcation analysis and limit cycle oscillation amplitude prediction methods applied to the aeroelastic galloping problem. Journal of Fluids and Structures 23 (7), 983–1011.